Available online at www.sciencedirect.com
ScienceDirect
International Journal of Mass Spectrometry 260 (2007) 177–184
International Journal of Mass Spectrometry
www.elsevier.com/locate/ijms

# Neuropeptide imaging on an LTQ with vMALDI source: The complete 'all-in-one' peptidome analysis

Peter D. Verhaert [a,b,c,d,*], Maria C. Prieto Conaway [e], Tonya M. Pekar [e], Ken Miller [e]

[a] *Analytical Biotechnology Laboratory, Delft University of Technology, Delft, The Netherlands*
[b] *BioMedical Research Center, University of Hasselt, Belgium*
[c] *Mass Spectrometry Laboratory, University of Liège, Belgium*
[d] *Flemish Interuniversity Institute of Biotechnology, Molecular Cell Biology Laboratory, Leuven, Belgium*
[e] *Thermo Electron Corporation, San Jose, CA, USA*

Received 22 June 2006; accepted 14 November 2006

**Abstract**

Direct tissue imaging was performed on dissected insect tissue using a MALDI ion trap to visualize endogenous neuropeptides. Coupling tissue imaging to tandem $MS^n$ allows for the identification of previously known species and the ability to identify new ones by *de novo* sequencing, as searchable databases for insects are sparse. Direct tissue imaging is an attractive technique for the study of neuropeptides as minimal sample preparation is required prior to mass spectrometry. We successfully identified neuropeptides present in the corpora cardiaca and allata of *Acheta domesticus* (the house cricket). Diagnostic fragments at low *m/z* were used to distinguish between lipids and neuropeptides. The distribution of peptides appears to be more differentially localized than that of phospholipids, which seem to be more evenly distributed within the tissue.


*Keywords:* MALDI MS imaging; Ion trap; $MS^n$; Neuropeptide

## 1. Introduction

Neurosecretion is a very important physiological phenomenon in the animal kingdom. It is one of the major systems with which cells, tissues, and organs communicate with one another throughout the body, and is generally accepted to be one of the main regulatory mechanisms with which the function of the various tissues and organs are harmonized within the multicellular organism [1].

Whereas the concept of neurosecretion dates from the first quarter of the previous century [2, see also 1], it was not until the advent of antibody technology and immunohistochemistry (IHC) some 50 years later, that neuroendocrinologists discovered a methodology to specifically localize neuropeptides at the tissue level. Early IHC work focused on localizing neurosecretory peptides in the main synthesis and storage/secretion sites of the nervous systems of many animal species (e.g., [3]). Many neuropeptides were immunolocalized in cerebral nuclei (e.g., the hypothalamus) and the immunoreactive peptide contained in nerve fibres could be traced running through the brain and extensively branching in neurohaemal (neurosecretory) organs, such as the pituitary (hypophysis) gland. The same IHC technology was further used to localize typical neuropeptides (or, at least, immunosimilar substances) at non-neuronal sites in the body, including intestinal, respiratory and reproductive epithelia, both in the same species that the peptide had originally been discovered in as well as in other species. It is in this context of heterologous use of antibodies for comparative study of neuropeptides across species that we became involved in this biological discipline (e.g., [4,5]). Being interested in evolution, we wanted to find out how far back in the phylogenetic tree vertebrate-type neuropeptides could be tracked. In brief, it is now common knowledge that most invertebrates share various neuropeptide families with vertebrate species.

Our invertebrate neuroendocrine model system for the past 20 years has been the insect brain–corpus cardiacum (CC) axis, equivalent to the mammalian brain–pituitary system, as was discovered in the 1940s. More than 50 different neuropeptide

* Corresponding author at: Laboratory for Analytical Biotechnology, Delft University of Technology, Department of Biotechnology, Julianalaan 67, 2628 BC Delft, The Netherlands. Tel.: +31 6 140 15 150; fax: +31 15 21 33 142.
*E-mail address:* p.d.e.m.verhaert@tudelft.nl (P.D. Verhaert).

1387-3806/$ – see front matter © 2006 Elsevier B.V. All rights reserved.
doi:10.1016/j.ijms.2006.11.008

pathways could be mapped in an insect species as primitive as a cockroach, particularly using heterologous peptide antibody IHC [6]. Obviously, the more heterologous the search, the more important specificity becomes. Whenever an unexpected 'exotic' immunolocalization of a neuropeptide needed to be proven, the classical approach, of peptide extraction and purification from its newly discovered source needed to be taken and was followed by peptide characterization and identification. Particularly when working with small specimens, such as insects, this process often involved the dissection of thousands of tissues, followed by months of tedious chromatography purifications of a single neuropeptide, in order to obtain enough material for peptide sequencing by Edman degradation (e.g., [7]).

Mass spectrometry (MS) truly revolutionized this field because of its higher sensitivity compared to Edman sequencing (femtomoles or less versus picomoles), but also because of its superior selectivity (peptide sequence information can be derived from mixtures in tandem MS systems). Instead of thousands of sacrificed insects and arduous peptide isolation and analysis work, today insect neuropeptide sequences can be derived from as little biological sample material as a single CC and even less [8].

Unfortunately, extraction of peptides from tissues destroys peptide localization and spatial information. This issue could only partly be solved by improving the resolution of the tissue microdissection prior to extraction, with different parts of the insect nervous system extracted separately (ultimately achieved with laser capture microdissection technology). A major step forward came 10 years ago when it became evident that neuropeptides could be directly analyzed from tissue by MALDI MS in so-called 'direct tissue MS' approaches, where the peptide-secreting tissue is introduced in the MS instrument in intact form. With novel direct-analysis MS (and MS/MS) instruments becoming accessible, we have been assessing several of them with the goal to develop the most complete peptidomics/peptide analysis system (e.g., [9]).

The ideal peptidome analysis system, would combine $MS^n$ sequencing capabilities with MS imaging technology, allowing direct tissue analysis of neuropeptide sequences without losing the spatial information which details a respective peptides' localization. A few years ago we analyzed our insect CC model in a typical MS imaging system (the matrix enhanced (ME) SIMS instrument developed at the Amsterdam AMOLF Institute). Our initial experiments on the ME SIMS apparatus indeed proved that various ions could be differentially localized in the insect retrocerebral complex, however, the system seemed to preferably demonstrate the localization of small phospholipid-derived ions (such as choline, cholesterol, diacylglycerol) and not true neuropeptide ions [10].

We here present our latest MS imaging results on insect CC neurosecretory tissue on a Finnigan™ LTQ™ ion trap MS system equipped with a vMALDI™ source (Thermo Electron Corp., CA, USA). They include our first successful experiments to localize and image multiple ions in the neuropeptide range in neuroendocrine tissue. Moreover, the $MS^n$ capabilities of the LTQ allowed us not only to generate peptide (precursor) ion images, but also to obtain MS/MS spectra from a single insect CC sample, which unequivocally proved their identity as neuropeptides.

## 2. Experimental

### 2.1. Materials

Adult house crickets (*Acheta domesticus*) were purchased (local pet shop) and segregated as males or females. Recrystallized MALDI matrices α-cyano-4-hydroxycinnamic acid (α-CHCA) and 2,5-dihydroxybenzoic acid (2,5-DHB) were purchased from Laser Biolabs (Cedex, France). Solvents used were acetonitrile LC–MS Chromasolv grade (Aldrich, WI, USA), trifluoroacetic acid (TFA) Sequanal grade, diluted to 0.1% aqueous (v/v) (Pierce Biotechnology, IL, USA), and 18 MΩ water (Millipore, MA, USA). Matrices were dissolved in 50/50 acetonitrile/0.05% TFA.

### 2.2. Tissue extraction and sample treatment

Crickets were decapitated and the corpora cardiaca (CC) and allata (CA) were dissected dry and rinsed in 250 mM sucrose aqueous solution.

For LC MS(/MS) analyses, 1 min organic extractions from CC and CA tissues were performed in 10 μl of 50/50 methanol/0.1% aqueous TFA. Separate 1 min extracts from five individual males and five individual females were pooled per sex for peptide identity and sequence confirmation.

For optimizing MALDI MS analysis parameters and MS imaging, a total of 11 female specimens were used. The fresh tissue was placed on a MALDI stainless steel surface (the tissue easily fitted within a 3 mm diameter MALDI sample well, see Fig. 5) and immediately either spotted or airbrushed (Aztek A470, Testors, Rockford, IL) with matrix solution. Matrix solutions employed included 5 mg/ml α-CHCA and either 50 or 150 mg/ml 2,5-DHB. The latter matrix preparation appeared to produce the better signal-to-noise and more analyte peaks in the spotted (dried droplet) samples. Therefore, a 150 mg/ml concentration of 2,5-DHB was selected for airbrushing matrix on to the tissue for MS imaging.

### 2.3. Mass spectrometry

To characterize the neuropeptide content of the cricket CC/CA tissue under investigation, a hybrid LTQ Orbitrap™ mass spectrometer [11] was employed to obtain high-resolution accurate mass MS and tandem MS information. For this, CC/CA tissue extracts were diluted 10-fold with a 2% acetonitrile/1% formic acid solution. Five microliters were injected on a commercial packed tip (New Objectives Biobasic C18, 300 Å, 5 μm particle size packing material; column dimensions 75 μm i.d. × 100 mm × 15 μm i.d. pulled silica tip). A gradient elution of 2% acetonitrile/0.1% formic to 50% acetonitrile/0.1% formic acid was conducted over 120 min at a flow rate of ∼300 nl/min measured at 50% acetonitrile/0.1% formic acid. A Surveyor™ MS pump with split flow was used to achieve the nanoflow gradient over the column (150 μl/min flow rate at pump).

Peptide ion isolation and collisional dissociation were achieved in the linear ion trap, and both precursor and product ions were detected in the Orbitrap. Full MS data were acquired at the 60,000 resolving power setting. Tandem MS data were acquired at the 7500 resolving power setting. A data-dependent method analyzing the monoisotopic peak of the six most intense ions in the full MS spectrum (as determined through Xcalibur™ software) was used, using automated dynamic exclusion of ions with a duration of 30 s existence on the exclusion list for ions within a 20 ppm window of the selected precursor.

For tissue imaging MS, a Finnigan LTQ ion trap instrument equipped with an intermediate pressure MALDI (vMALDI) source was used [12]. The supplied acquisition software (LTQ Tune Plus™) was modified to allow laser desorption in a raster pattern over the tissue to create two- and three-dimensional MS images. The various analytes were viewed and their distribution mapped with custom imaging visualization software (Thermo Electron Corp., CA, USA). The vMALDI source was equipped with a nitrogen laser (337 nm) coupled to the mass spectrometer through a fibre optic cable. The laser spot at the sample was approximately 100 μm in diameter. Helium was used as the collision gas during collision induced dissociation (CID). Tissue imaging experimental methods were implemented through Xcalibur in a complete autonomous mode.

An automated data-dependent experiment (Nth Double Play) was collected off tissue, with 1 MS scan followed by 25 MS/MS scans. This experiment was carried out with plate motion controlled by crystal recognition software (CPS), i.e., in this experiment no attempt was made to retain the spatial information of the peptides as would be done in a typical imaging experiment. CPS was used in combination with the Auto Spectral Filter (ASF) algorithm to set a signal intensity threshold.

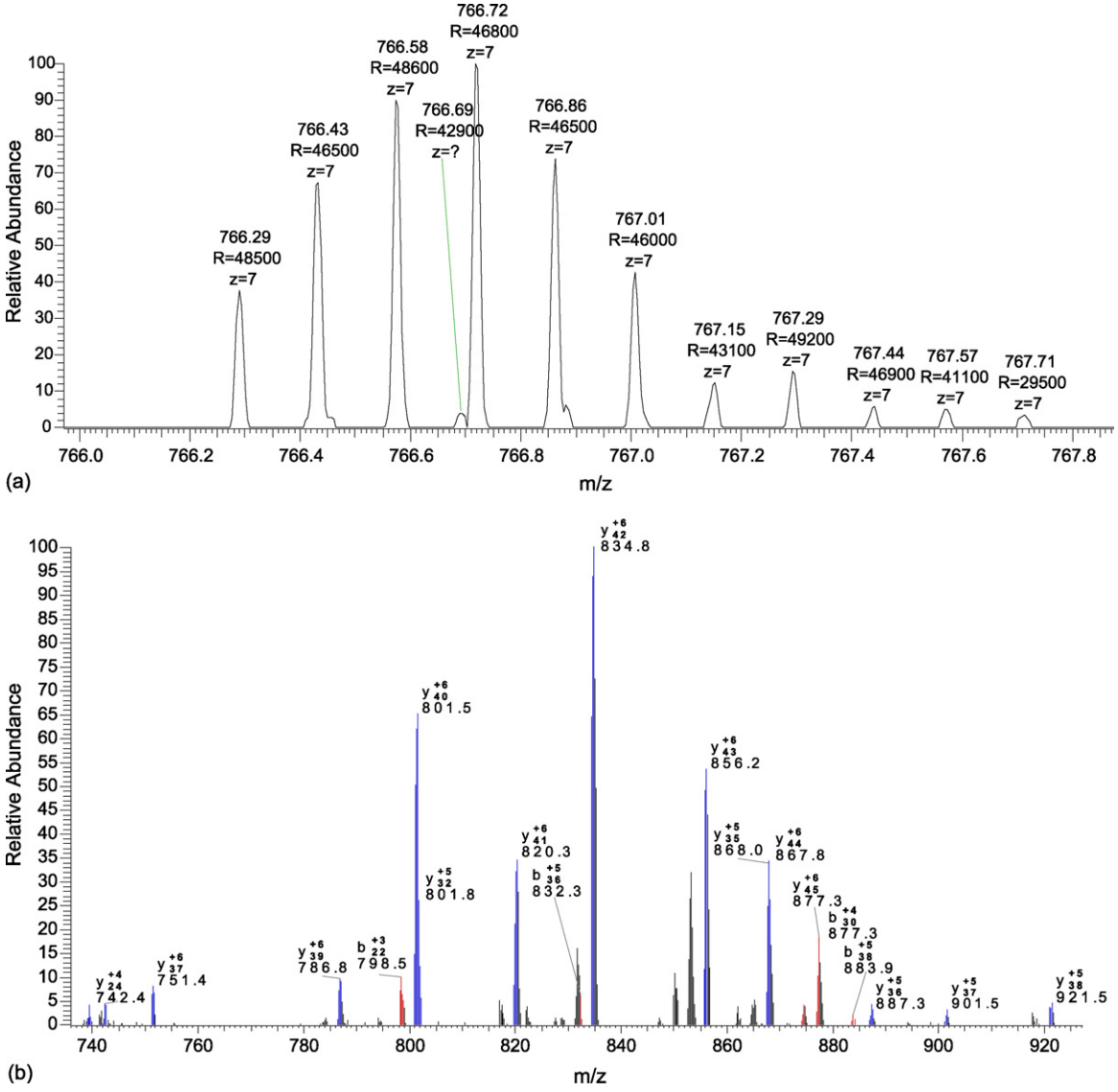


Fig. 1. LTQ Orbitrap data of a previously described Acheta neuropeptide with sequence TGAQSLSIVAPLDVLRQRLMNELNRRRMRELQGSRIQQNRQLLTSI, identified as DIUH_ACHDO Diuretic hormone (Diuretic peptide) (DP) by BioWorks database search. (a) MS of 7+ charge ion at *m/z* 766.29 and (b) MS/MS with sequence annotation.

Data were acquired using Automatic Gain Control (AGC), in which a prescan determines the number of laser shots required to optimally fill the ion trap per scan. This corresponded to 1 laser shot for the MS and 10 laser shots for the MS/MS scans at the laser power selected for the acquisition. In addition, 2 and 12 microscans were averaged for the MS and the MS/MS scans, respectively. The MALDI fragmentation data were searched using BioWorks™ 3.3 (SEQUEST®) database search algorithm. An *A. domesticus* (house cricket) database was downloaded in FASTA format from the Expert Protein Analysis System (ExPASy) organization, as were those from related orthopteroid insect species (field cricket *Gryllus*), and migratory and desert locust, respectively (*Locusta* and *Schistocerca*).

Pulsed *Q* dissociation (PQD) [13] lowers the low mass cutoff in the LTQ ion trap to 50 amu and was used to monitor low mass diagnostic ions from phospholipids. In PQD the activation *Q* value is pulsed from high to low, with a delay time in between to allow energetic collisions of the ions. The activation *Q* is kept constant in regular CID.

## 3. Results and discussion

### 3.1. Sample preparation for peptide detection

Tissue samples that were washed in isotonic sucrose solution after dissection showed reduced interfering salts and produced higher quality MS spectra than samples which were rinsed in water (data not shown). Hence the sucrose rinse was preferred over the water or aqueous ethanol wash, as previously used [10]. The use of aqueous ethanol rinses is a common practice in tissue MS imaging to wash excess lipids and salts from tissues such as the mouse brain [14,15].

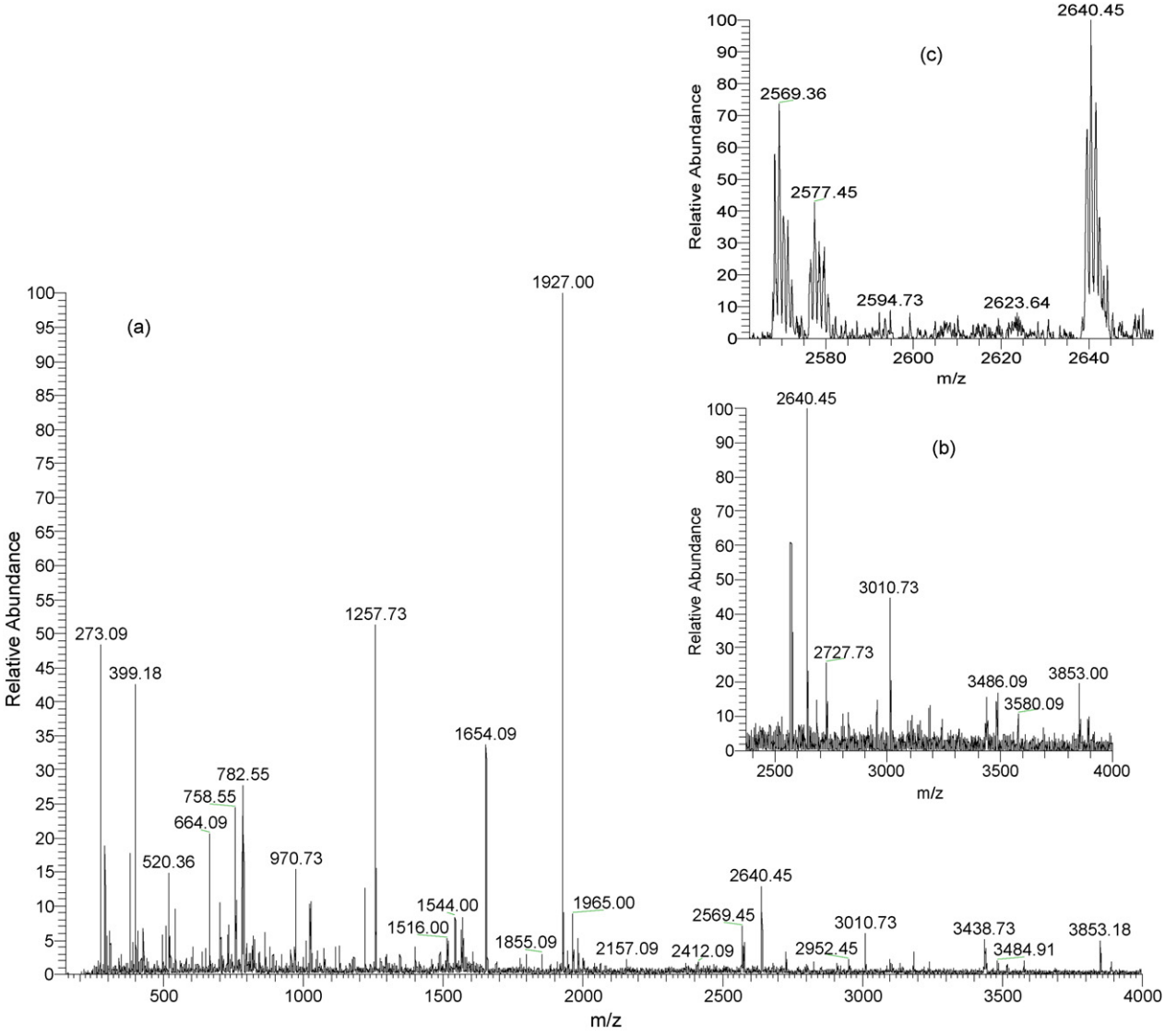


Fig. 2. (a) Full direct tissue MS of house cricket corpus cardiacum (dried droplet matrix application: 2× 0.5 μl 2,5-DHB [150 mg/ml]). (b) Expanded region for ions above *m/z* 2500. (c) Higher zoom of spectrum, showing isotopic resolution above *m/z* 2500 (acquisition at normal scan rate). It is noteworthy that none of the major peptide ion peaks showing up in this spectrum represents any of the previously described *Acheta* neuropeptide sequences, suggesting detection of a whole series of novel peptide sequences.

All samples were tested with two different matrices: αCHCA and 2,5-DHB at two concentrations. It was established that, in all cases the higher concentrated 2,5-DHB solution produced the best spectra. The 50/50 acetonitrile/aqueous TFA solvent used in the matrix is compatible with the extraction (and preservation) of hydrophilic peptides [16].

### 3.2. Neuropeptide identification by LTQ Orbitrap MS

Nanoscale LC LTQ Orbitrap MS yielded over 500 different peptide ion species. This is comparable with our study in cockroach CC, where 6–10 times more peptides can be visualized with appropriate nano-LC separation combined with MS compared to direct tissue MALDI profiling [17]. As in our cockroach study, the vast majority of the detected peptide peaks cannot be attributed to previously described sequenced neuropeptides, thus suggesting the occurrence of many novel peptides in the insect under investigation. Even more, none of the major peptide peaks detected directly from tissue in the MALDI analysis (Fig. 2) represents any of the published *Acheta* neuropeptides. LC MS(/MS) Orbitrap analysis of the samples, however did reveal, at least, one of the known peptides (Fig. 1), with *m/z* 5357.97 (cricket diuretic peptide: TGAQSLSIVAPLDVLRQRLMNELNRRRMRELQGSRIQQNRQLLTSI). Its sequence could be confirmed by MS/MS and database search with BioWorks. The mass accuracy of the Orbitrap from this peptide was calculated at 5 ppm, and by comparing the mass measurements of the peptide peaks overlapping between Orbitrap and vMALDI we can estimate the mass accuracy of the direct tissue vMALDI MS analyses to be in the range of 20–120 ppm.

### 3.3. MALDI mass spectral data

Freshly dissected tissue obtained after sucrose wash and with 150 mg/ml DHB dried droplet matrix application showed the best spectra of the three different matrix solutions tested (Fig. 2). Data were acquired under normal scan rate, which maintains isotopic resolution of the ions to *m/z* 4000. The ions in the MS spectrum suggest small endogenous peptides. Partial *de novo* sequencing confirmed that these were indeed peptides.

Direct tissue data-dependent MS and MS/MS experiments (1 MS scan followed by 25 MS/MS scans), showed MS spectra (Fig. 3a) that varied in ion abundance and showed less ions above *m/z* 3000 as compared to Fig. 2a. This is probably a reflection of the finer DHB crystals of this sample (less analyte incor-

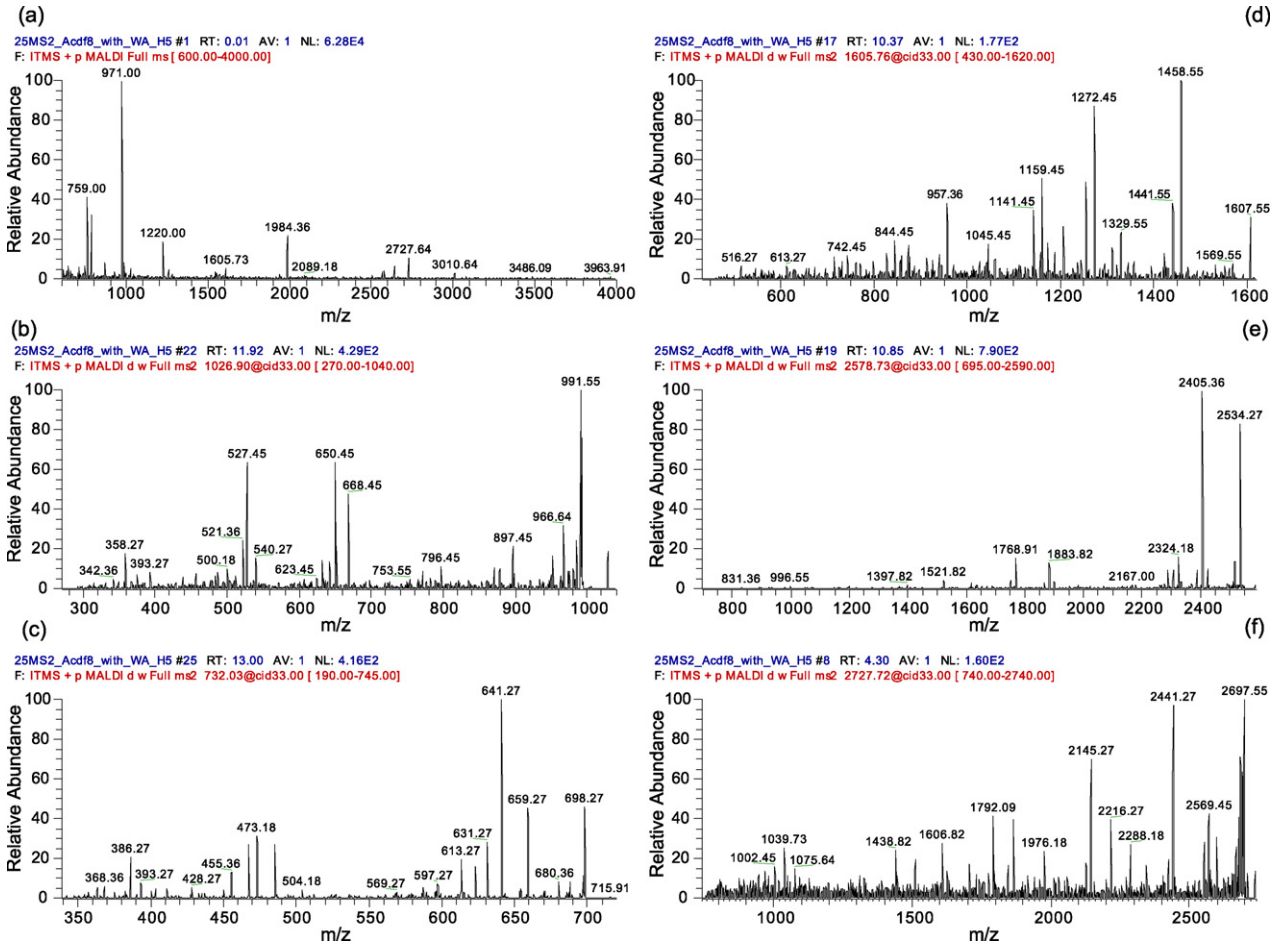


Fig. 3. Automated data-dependent experiment directly of tissue: 1 MS followed by 25 MS/MS. In contrast to the matrix application in Fig. 2, DHB matrix on this sample was "airbrushed". (a) Full scan MS. (b–f) MS/MS fragmentation spectra showing characteristic spacing suggestive of amino acid residues. Singly charged precursor masses include: (b) *m/z* 1026.9; (c) *m/z* 732.0; (d) *m/z* 1605.8; (e) *m/z* 2578.7; (f) *m/z* 2727.7.

poration for aerosolized matrix application) and only one scan averaged as compared to the dried droplet sample with several averaged scans. The total number of laser shots per scan was 2 (for the MS) and 120 (for each MS/MS). All data acquisition filters were used (crystal positioning system, CPS; auto spectral filter, ASF; and automatic gain control, AGC) with a typical data-dependent experiment taking less than 15 min to complete. The high concentration, aerosolized matrix application resulted in finely nebulized DHB crystals, much unlike the typical needle-like DHB crystals obtained by the dried droplet procedure. It is clear that peptide analyte diffusion during matrix crystallization is much reduced in this nebulizing versus dried droplet matrix application. Searching the fragmentation data with BioWorks ("No Enzyme Search", since cricket propeptide conversion enzyme specificities remain poorly understood) against the *Acheta* database did not yield any automatic peptide identification. As this database is only sparsely populated, the database was expanded with sequences from related species, *Gryllus*, *Locusta*, and *Schistocerca*, but no hits were detected. It is obvious that the *in silico* generation of peptides by a sequence specific protease such as trypsin is much less complicated than applying all known propeptide conversion enzyme rules to an entire protein sequence database. Therefore, rather than focusing on the animal taxonomy, it could be beneficial here to search against specific well cured (neuro)peptide sequence databases, such as SwePep [18].

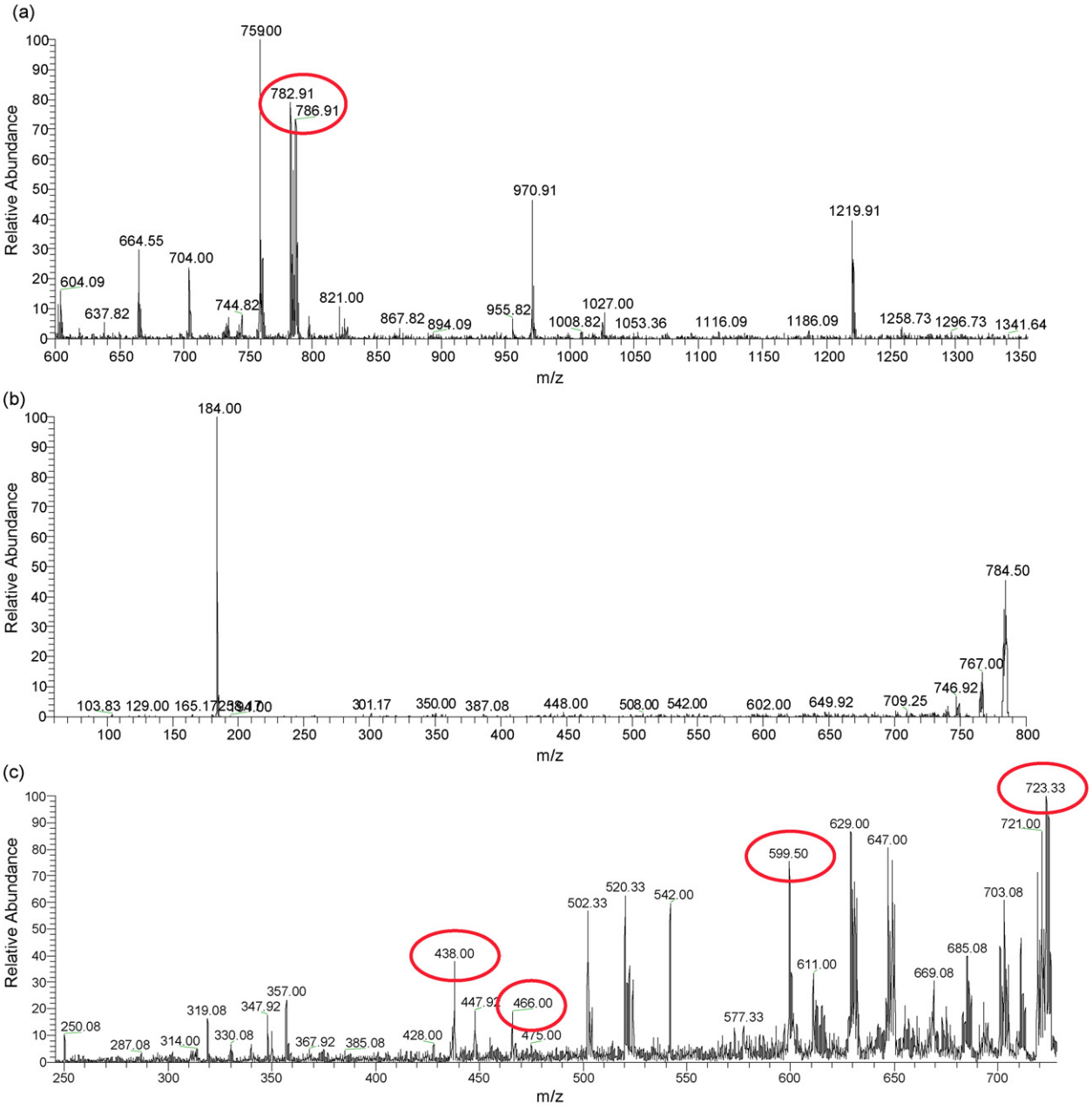


Fig. 4. PQD ion activation technique for determination of low mass diagnostic lipid ions. (a) Full MS, circled ions are *m/z* 782.9–786.9. (b) PQD fragmentation with precursor isolation at 784 indicates phospholipid diagnostic fragment at *m/z* 184. (c) PQD fragments above *m/z* 184 show neutral losses typical of phospholipids (in red).

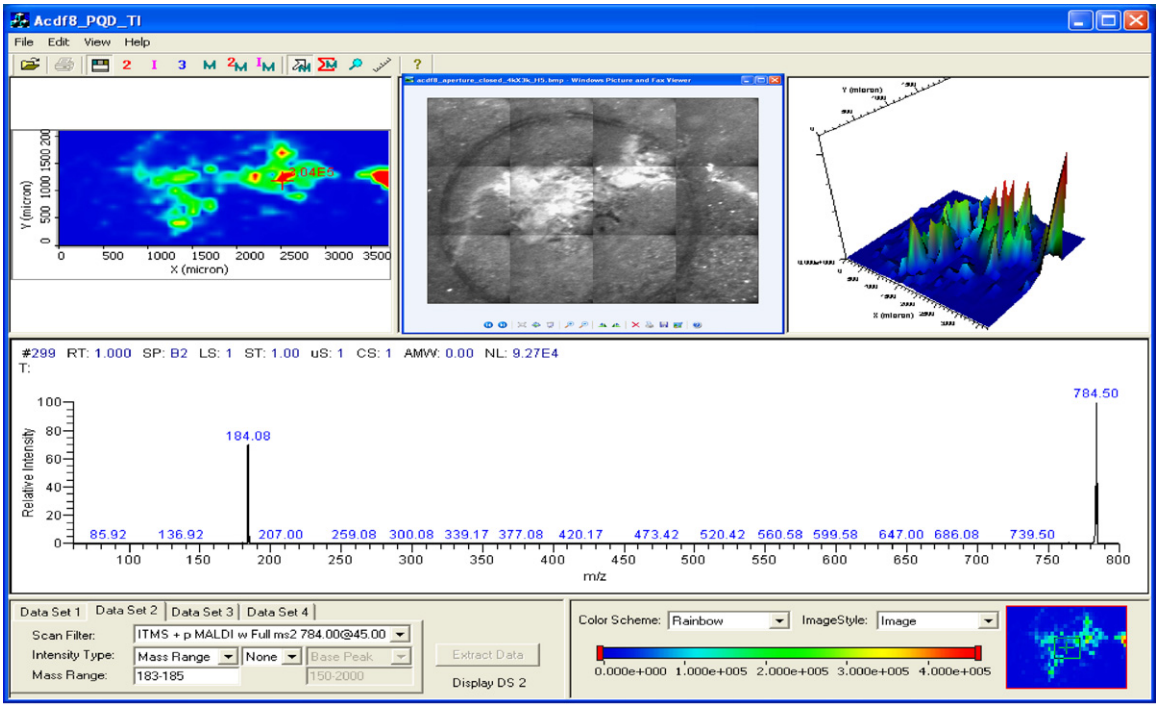


Fig. 5. vMALDI LTQ imaging of cricket CC–CA tissue, as shown from the MALDI Data Browser window. The typical phospholipid fragment ion at *m/z* 184 is mapped. Top panel shows the spatial distribution of this fragment in a two-dimensional image (left), the optical image (center) of the tissue on a stainless steel surface with matrix (the circle around the tissue is 3 mm in diameter; orientation: two CA visible on left side, both longer CC extending to the right), and a three-dimensional image (right). The *xy* axes in the MS images are distances along the tissue in micron, whereas the *z*-axis in the three-dimensional image is relative abundance. The bottom panel shows the spectrum at the cursor in the two-dimensional image, placed at a high intensity (red) area.

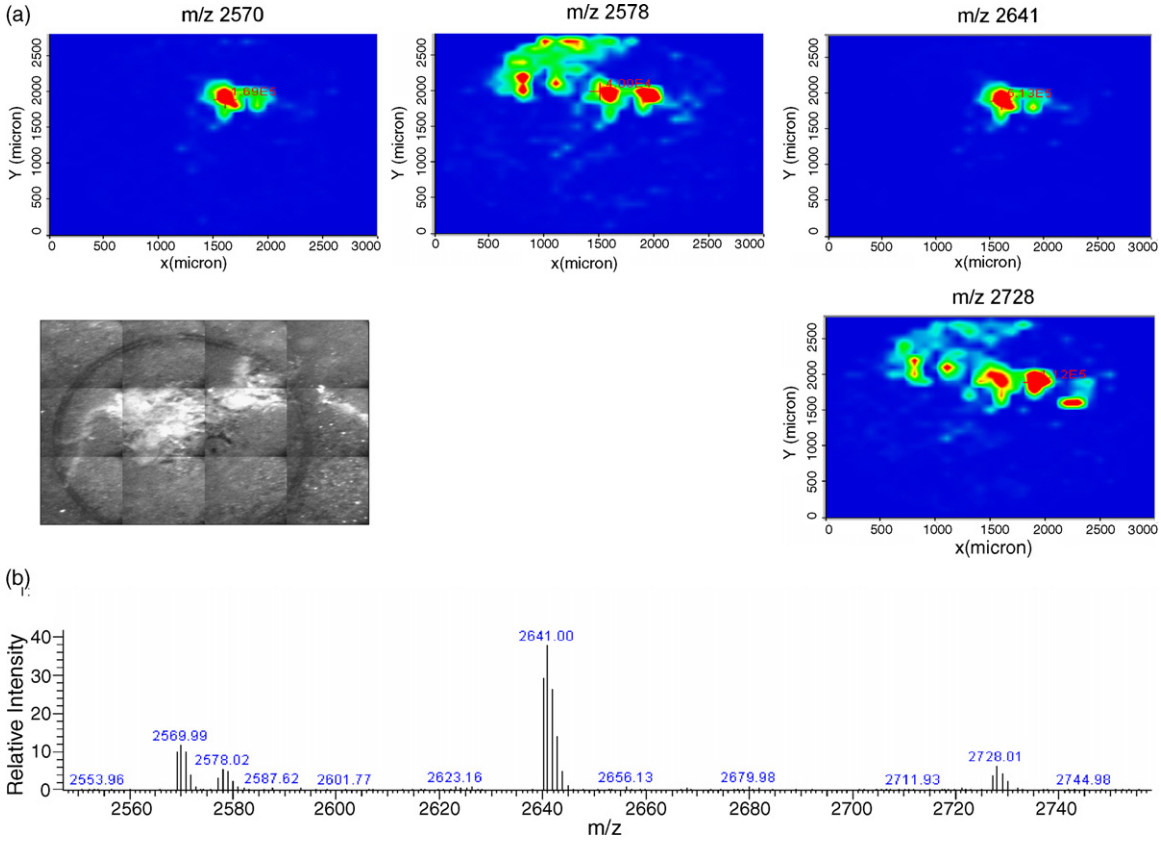


Fig. 6. (a) LTQ vMALDI MS images of house cricket CC/CA, showing distribution of different peptide ions within the tissue complex. (b) MS spectrum with the four selected peptide ions mapped in the MS images.

Phospholipid ions, which occur in high abundance in brain tissue of most organisms, typically appear in the 700–900 mass range, with dimer adducts occurring around *m/z* 1500. PQD was effectively used to monitor the low mass region in order to differentiate peptides from lipids. Fig. 4 shows the PQD fragmentation spectrum for *m/z* 784 ion, where a very prominent fragment ion at *m/z* 184 is indicative of a phosphatidylcholine or sphingomyelin [12]. Neutral losses of 59 and 124 are typical of these polar lipids; the appearance of MS ions at *m/z* 723.3 and 599.5 could possibly identify one of the species as PC (16:0, 18:1) with precursor $[M+Na]+$ at 782.6. This most likely occurs due to inclusion of *m/z* 782.6 when isolating *m/z* $784 \pm 1.5$ amu. The difference of 28.00 amu between the ions at *m/z* 466.0 and 438.0 can be attributed to $C_2H_4$, the difference in the length between two saturated fatty acid chains. The complex spectrum in Fig. 4c agrees with fragmentation from more than one precursor, possibly those at *m/z* 782.5, 784, and 785.5, plus possibly isoforms [19]. Using the nitrogen rule, precursors with even *m/z* ($[M+H]+$) can be assigned to phospholipids bearing a single nitrogen atom, while those with odd *m/z* can be assigned to lipids with two nitrogens, such as sphingomyelins. Identifying every single ion in the fragmentation spectrum is beyond the scope of this work. However, we have demonstrated that fragmentation with PQD activation can quickly determine the presence of phospholipids by monitoring *m/z* 184.

### 3.4. MALDI tissue imaging

The variability of ion distribution within the tissue is displayed in Figs. 5 and 6 for the same tissue sample. The different MS images displayed, correspond to either phospholipids (Fig. 5), peptides, or a mixture of both (Fig. 6). Phospholipids (as *m/z* 184) appear to be evenly distributed within the cricket CC–CA tissue. All the MS images in Fig. 6 display a more distinct bi-lobe structure, with the two images at *m/z* 2570 and 2641 showing distribution of the particular ion exclusively within these substructures (the CC, extending to the right in the image). This is reminiscent of the general structure of orthopteroid CC, which have an intrinsic glandular part and a peptide storage part. Most peptides in the MS spectrum were checked by partial manual sequencing to confirm their peptidic nature. For example, the difference between *m/z* 2570 and 2641 corresponds to the loss of an Ala residue (−71); that between 2728 and 2641 is a loss of a Ser residue (−87).

## 4. Conclusion

Optimization of sample treatment is crucial for the successful analysis of endogenous neuropeptides of tissue samples. Each tissue system and each instrument platform might present different challenges that need to be addressed for each particular imaging study. These include sample treatment after dissection, storage conditions if not analyzing immediately, wash conditions, choice of matrix, matrix concentration, and matrix application, among others.

Fresh samples were critical for the successful detection of endogenous neuropeptides of tissue by imaging mass spectrometry. In particular, the isotonic sucrose wash followed by high concentration of nebulized DHB provided optimal conditions. The LTQ with vMALDI source has been demonstrated as a viable platform for neuropeptide tissue imaging, allowing discrimination of substructures within tissue as small as 1.5 mm × 3 mm approximate size, and at the same time allowing $MS^n$ peptide sequence analyses.

Future goals are to increase the resolution of the technique by rastering at smaller increments. We have preliminary results (test samples, 10 mm × 10 mm size) that demonstrate reducing raster sampling to 20 μm (as opposed to 100 μm) improves the MS image resolution substantially, as has been previously reported by Sweedler's group [20]. Software improvements, such as alignment of optical and MS images, and incorporation of various analytes into one image, could greatly benefit the analysis of tissue samples with this technique.

We are currently analyzing the large amount of MS/MS data generated by LTQ Orbitrap from the cricket CC–CA organic liquid extractions, in order to increase the percentage of full peptide identifications by *de novo* sequencing.

## Acknowledgement

This paper is dedicated to Prof. Dr. Gijs van Dedem who was promoted emeritus this year.

## References

[1] B. Scharrer, Am. Zool. 30 (1990) 887.
[2] C.C. Speidel, Papers Dept. Mar. Biol. Carnegie Inst. Wash. 13 (1919) 1.
[3] F. Vandesande, K. Dierickkx, Cell Tissue Res. 179 (1976) 289.
[4] P. Verhaert, S. Marivoet, F. Vandesande, A. De Loof, Cell Tissue Res. 238 (1984) 49.
[5] D. Schols, P. Verhaert, R. Huybrechts, H. Vaudry, S. Jégou, A. De Loof, Histochemistry 86 (1987) 345.
[6] P. Verhaert, PhD thesis, University of Leuven, Belgium, 1987, 241 pp.
[7] K. Spittaels, P. Verhaert, C. Shaw, R.N. Johnston, B. Devreese, J. Van Beeumen, A. De Loof, Insect Biochem. Mol. Biol. 26 (1996) 375.
[8] P. Verhaert, A. De Loof, F. Vandesande, R. Bordoli, J. Hoyes, Proceedings of the 45th ASMS Conference on Mass Spectrometry and Allied Topics, 1997 (extended abstract).
[9] P. Verhaert, S. Uttenweiler-Joseph, M. de Vries, A. Loboda, W. Ens, K.G. Standing, Proteomics 1 (2001) 118.
[10] L.A. McDonnell, S.R. Piersma, M.A.F. Altelaar, T.H. Mize, S.L. Luxembourg, P.D.E.M. Verhaert, J. van Minnen, R.M.A. Heeren, J. Mass Spectrom. 40 (2005) 160.
[11] A. Makarov, E. Denisov, A. Kholomeev, W. Balschun, O. Lange, K. Strupat, S. Horning, Anal. Chem. 78 (2006) 2113.
[12] T. Garrett, R.A. Yost, Anal. Chem. 78 (2006) 2465.
[13] J. Schwartz, U.S. Patent No. 6,949,743.
[14] B.J. Xu, R.M. Caprioli, M.E. Sanders, R.A. Jensen, J. Am. Soc. Mass Spectrom. 13 (2002) 1292.
[15] P. Chaurand, S.A. Schwartz, D. Billheimer, B.J. Xu, A. Crecelius, R.M. Caprioli, Anal. Chem. 76 (2004) 1145.
[16] P. Chaurand, S.A. Schwartz, R.M. Caprioli, Anal. Chem. 76 (2004) 86A.
[17] P.D. Verhaert, G. Schwarz, A.R. Kroon, J.A. Langridge, J.C. Vissers, Proceedings of the 54th ASMS, Seattle, WA, 2006.
[18] M. Falth, K. Skold, M. Norrman, M. Svensson, D. Fenyo, P.E. Andren, Mol. Cell. Proteomics 5 (2006) 998.
[19] T.J. Garrett, et al., Int. J. Mass Spectrom. 260 (2007) 166–176.
[20] J.C. Jurchen, S.S. Rubakhin, J.V. Sweedler, J. Am. Soc. Mass Spectrom. 16 (2005) 1654.